Quantifying the Mechanisms of Atmospheric Circulation Response to Greenhouse Gas Increases in a Forcing–Feedback Framework

PENGFEI ZHANG,[a,b] GANG CHEN,[a] AND YI MING[c]

[a] *Department of Atmospheric and Oceanic Sciences, University of California, Los Angeles, Los Angeles, California*
[b] *Department of Meteorology and Atmospheric Sciences, Pennsylvania State University, University Park, Pennsylvania*
[c] *NOAA/Geophysical Fluid Dynamics Laboratory, Princeton, New Jersey*

(Manuscript received 5 October 2020, in final form 8 March 2021)

ABSTRACT: While there is substantial evidence for tropospheric jet shift and Hadley cell expansion in response to greenhouse gas increases, quantitative assessments of individual mechanisms and feedback for atmospheric circulation changes remain lacking. We present a new forcing–feedback analysis on circulation response to increasing CO_2 concentration in an aquaplanet atmospheric model. This forcing–feedback framework explicitly identifies a direct zonal wind response by holding the zonal mean zonal wind exerting on the zonal advection of eddies unchanged, in comparison with the additional feedback induced by the direct response in zonal mean zonal wind. It is shown that the zonal advection feedback accounts for nearly half of the changes to the eddy-driven jet shift and Hadley cell expansion, largely contributing to the subtropical precipitation decline, when the CO_2 concentration varies over a range of climates. The direct response in temperature displays the well-known tropospheric warming pattern to CO_2 increases, but the feedback exhibits negative signals. The direct response in eddies is characterized by a reduction in upward wave propagation and a poleward shift of midlatitude eddy momentum flux (EMF) convergence, likely due to an increase in static stability from moist thermodynamic adjustment. In contrast, the feedback features a dipole pattern in EMF that further shifts and strengthens midlatitude EMF convergence, resulting from the upper-level zonal wind increase seen in the direct response. Interestingly, the direct response produces an increase in eddy kinetic energy (EKE), but the feedback weakens EKE. Thus, the forcing–feedback framework highlights the distinct effect of zonal mean advecting wind from direct thermodynamic effects in atmospheric response to greenhouse gas increases.

KEYWORDS: Atmospheric circulation; Climate change; Eddies; Feedback; General circulation models; Hadley circulation

1. Introduction

It is well recognized that the zonally averaged global atmospheric circulation will experience significant changes in response to greenhouse gas increases. In association with the tropospheric warming and stratospheric cooling in response to CO_2 increases, an expansion of the Hadley cell has been found in both the observations and future climate projections (e.g., Lu et al. 2007; Hu and Fu 2007; Previdi and Liepert 2007; Seidel et al. 2008; Birner 2010; Ceppi and Hartmann 2013; Tao et al. 2016; Grise and Davis 2020), and the midlatitude jet streams and storm tracks are predicted to shift poleward under future climate warming (e.g., Yin 2005; Lorenz and DeWeaver 2007; Lu et al. 2008; Kidston and Gerber 2010; Wu et al. 2011; Chang et al. 2012; Barnes and Polvani 2013; Simpson and Polvani 2016; Mbengue and Schneider 2017). Together with the increased atmospheric water vapor content in a warming climate, these circulation responses to greenhouse gas increases could lead to profound changes in the hydrological cycle (e.g., Chou and Neelin 2004; Held and Soden 2006; Scheff and Frierson 2012; Lau and Kim 2015; Norris et al. 2019). While a large number of studies have investigated global atmospheric circulation changes in a warming climate, quantitative assessments of individual mechanisms and feedback to the circulation changes are still lacking (Shaw 2019; Held 2019). In this paper, we will present a new forcing–feedback perspective for the zonal mean zonal wind in response to greenhouse gas increases analogous to the climate sensitivity framework developed for surface temperature.

The mechanisms for the circulation changes in a warming climate can be roughly divided into two interrelated aspects [see reviews by Vallis et al. (2015) and Shaw (2019)]. The first one is focused on the effects of robust thermodynamic characteristics of greenhouse gas increases on the Hadley cell circulation. Held (2000) made a scaling argument for the width of the Hadley cell, in which the width is determined by the latitude where the thermally forced Hadley cell becomes baroclinically unstable. Given the increased static stability or the tropopause height rise under global warming (e.g., Manabe and Wetherald 1967), this scaling argument predicts that the increased static stability or lifted tropopause would lead to an expansion of the Hadley cell. This is supported by many modeling studies in which the static stability or tropopause of a climate model is perturbed (Williams 2006; Lorenz and DeWeaver 2007; Frierson 2008; Mbengue and Schneider 2017). The other perspective is centered on what determines the latitudes of midlatitude eddy-driven jets by studying the changes in the spatiotemporal properties of baroclinic eddies. The poleward shift of midlatitude jets has been attributed to changes to eddy phase speed (Chen et al. 2007, 2008), eddy length scale (Kidston et al. 2011), barotropic instability (Kidston and Vallis 2012), the type and frequency of Rossby wave breaking (Rivière 2011), or the reflection of baroclinic waves (Lorenz 2014).

Corresponding authors: Pengfei Zhang, pfz5053@psu.edu; Gang Chen, gchenpu@atmos.ucla.edu

DOI: 10.1175/JCLI-D-20-0778.1

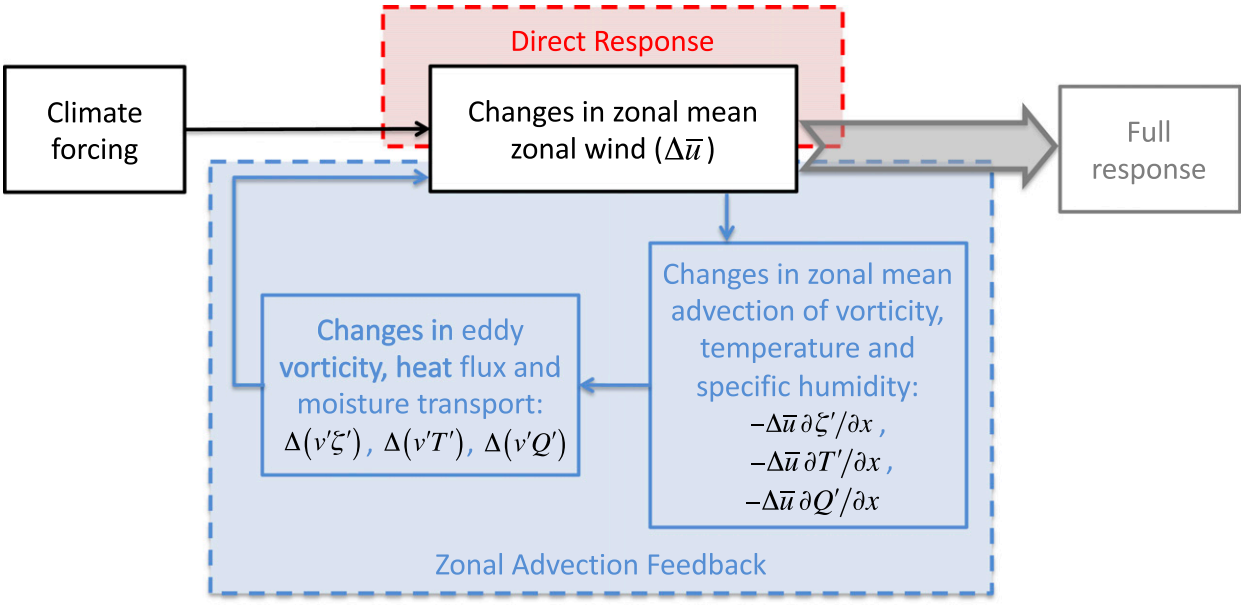

FIG. 1. Schematic of a forcing–feedback framework for the zonal mean zonal wind response to climate forcing. The changes in zonal mean zonal wind, induced by climate forcing (e.g., greenhouse gas increases), can alter the zonal advection of eddies and associated eddy fluxes of vorticity, heat, and water vapor, which, in turn, provide feedback to the zonal wind changes. The zonal wind changes without the zonal advection feedback are referred to as the direct response. The direct response plus the zonal advection feedback gives the full response to climate forcing.

This line of research is often related to the impacts of the Antarctic ozone hole on the tropospheric jet [see the review by Thompson et al. (2011)], in which changes in static stability or tropopause height are relatively small. Furthermore, changes in the Hadley cell and midlatitude eddy-driven jets are often correlated (Waugh et al. 2018). Thus, the complicated interactions between the tropics and extratropics and between the zonal circulations and baroclinic eddies prevent a simple explanation of the circulation response to greenhouse gas increases.

Compared with the traditional diagnosis of eddy–zonal flow interactions, Chen et al. (2020, hereafter CZL20) developed a unified forcing–feedback framework in which the interactions between the westerly jet and synoptic eddies are synthesized by a zonal advection feedback (see section 2 and the schematic in Fig. 1). This may be related to an initial-value large-ensemble approach used to understand the transition of atmospheric circulation from an equilibrated state to a new one for an instantaneous change to climate forcing in comprehensive climate models (e.g., Wu et al. 2012; Chemke and Polvani 2020) or idealized ones (e.g., Chen et al. 2013; Sun et al. 2013; Lu et al. 2014). In the early stage of the transition when the changes in zonal wind are small, it is expected that the feedback due to zonal wind changes plays a minor role compared with that in the equilibrated state. The forcing–feedback framework is designed to disable the zonal wind feedback so as to isolate the early stage of circulation changes, called the direct response, as compared with the later stage when the feedback makes a larger contribution. In the present study, we employ this forcing–feedback framework to quantify the direct response in zonal wind and the circulation feedback using an aquaplanet model so as to extend the dry atmospheric dynamical core used in CZL20 to a more realistic model with a hydrological cycle and thermodynamic effects of water vapor.

This paper is organized as follows: section 2 introduces the forcing–feedback framework and the overriding approach. Section 3 describes the model setup, experiment design, and the evaluation of the approach. In section 4, we compare the direct response with the contribution of the zonal advection feedback in the zonal mean circulation responses to quadrupling CO_2. Section 5 further investigates the relative contributions of the direct response and circulation feedback among a range of climates (with a quarter, half, double, and quadruple the preindustrial CO_2 concentration, respectively). Section 6 discusses the eddy mechanism in the direct response and zonal advection feedback. Finally, the conclusions are summarized in section 7.

2. Forcing–feedback framework

a. *The direct response to climate forcing versus zonal advection feedback*

As described in CZL20, the zonal wind response to climate change can be quantified in a forcing–feedback framework for zonal mean zonal wind similar to the climate sensitivity framework for global mean surface temperature (Roe 2009). In this framework, the zonal circulation response to climate forcing can be understood in a two-step procedure, as illustrated in Fig. 1. The first step computes the direct response in zonal circulation, when the climate forcing (e.g., greenhouse gas increases) is applied to the atmosphere with the zonal mean

zonal wind acting on the zonal advection of vorticity, temperature, and moisture being held the same as the undisturbed atmosphere. This step is designed to disable the influence of the direct response in zonal wind on the zonal advection of eddies [e.g., the increased eastward propagation of eddies due to the zonal wind acceleration as proposed in Chen et al. (2007)], and thus it is likely dominated by the thermodynamic effects of greenhouse gas increases. We will refer to the influence of the direct response in zonal mean zonal wind on the zonal advection of eddies as the zonal advection feedback (hereafter, zonal advection feedback for short). In the second step, the zonal advection feedback is calculated by imposing the direct response in zonal mean zonal wind from the first step to the zonal advection of eddies, and thus one can obtain additional changes in zonal circulation due to changes in eddy vorticity, temperature, and moisture fluxes (e.g., the eddy response to a faster jet); the additional changes in zonal wind will be further applied to the zonal advection of eddies to produce more changes to eddy fluxes. We integrate the model until a new equilibration between zonal wind and eddy fluxes is reached. As such, the forcing–feedback framework divides the zonal mean circulation response to climate change into two components: 1) the direct zonal wind response to the climate forcing by holding the zonal mean zonal wind exerting on the zonal advection of eddies undisturbed, and 2) additional feedback induced by the changes in zonal mean zonal wind through the zonal advection feedback.

Mathematically, let us denote the zonally averaged zonal wind in a vector form as Z ($\mathrm{m\,s^{-1}}$), whose length is the number of latitudinal grid points times the number of vertical levels used to discretize the atmosphere. In the time average, we could write an equation for zonal-mean zonal wind as (e.g., Ring and Plumb 2008)

$$\mathbf{MZ} = \mathbf{E}, \tag{1}$$

where $\mathbf{M}$ ($\mathrm{s^{-1}}$) describes all the processes for the zonally symmetric dynamics, including the horizontal and vertical advection and the thermal and frictional damping rates. The term $\mathbf{E}$ ($\mathrm{m\,s^{-2}}$) has the same dimension of $\mathbf{Z}$, representing all the eddy terms that are not resolved in the zonally symmetric dynamics. Since both $\mathbf{Z}$ and $\mathbf{E}$ are denoted by vectors, $\mathbf{M}$ is a square matrix that contains both local and remote relations between $\mathbf{Z}$ and $\mathbf{E}$. We will assume that $\mathbf{M}$ does not change with climate forcing.

In response to an effective zonal momentum forcing $\mathbf{F}$ induced by climate forcing (e.g., greenhouse gas increases), the changes in zonal mean wind are

$$\Delta\mathbf{Z} = \mathbf{M}^{-1}(\mathbf{F} + \Delta\mathbf{E}). \tag{2}$$

Here $\Delta\mathbf{E}$ describes all the eddy changes resulting from climate forcing, which can be further expanded to the first order of the zonal wind changes as

$$\Delta\mathbf{E} = \Delta\mathbf{E}_0 + (\partial\mathbf{E}/\partial\mathbf{Z})\Delta\mathbf{Z}, \tag{3}$$

where $\Delta\mathbf{E}$ are the eddy changes independent of zonal wind changes, and $\partial\mathbf{E}/\partial\mathbf{Z}$ is a square matrix that measures the spatial pattern of zonal advection feedback. Unlike the simple thermal or mechanical forcing used in previous studies (e.g., Ring and Plumb 2008; Hassanzadeh and Kuang 2016; CZL20), the computation of the effective zonal momentum forcing F for realistic climate change scenarios is challenging. However, since the feedback depends on the changes in zonal wind [$(\partial\mathbf{E}/\partial\mathbf{Z})\Delta\mathbf{Z}$ in Eq. (3)], the direct response may be thought of as the circulation response to climate forcing in the early stage of the transition from an equilibrated state to a new one for an instantaneous change to climate forcing in the initial-value large-ensemble approach, whereas the feedback becomes more important at a later stage when the zonal wind undergoes substantial changes.

The direct response in zonal wind is given by excluding the influence of zonal wind changes on the eddies:

$$\Delta\mathbf{Z}_0 = \mathbf{M}^{-1}(\mathbf{F} + \Delta\mathbf{E}_0). \tag{4}$$

It is noteworthy that the direct response here differs from a zonally symmetric response to given mechanical or thermal forcing discussed in the literature (e.g., Haynes et al. 1991; Kushner and Polvani 2004; Ring and Plumb 2008; Sun et al. 2013), because it may include the effect of the eddy changes that are independent of zonal wind changes, $\Delta\mathbf{E}_0$ (e.g., due to changes in static stability). Substituting Eq. (3) into Eq. (2) and after some rearrangements, the full response in zonal wind is related to the direct response as

$$\Delta\mathbf{Z} = (\mathbf{I} - \mathbf{M}^{-1}\partial\mathbf{E}/\partial\mathbf{Z})^{-1}\Delta\mathbf{Z}_0, \tag{5}$$

where $\mathbf{I}$ is an identity matrix.

More detailed formulations of this forcing–feedback framework and the comparison between the jet sensitivity and climate sensitivity were described in detail in CZL20. Similar to climate sensitivity, one can compute the feedback matrix, $\mathbf{M}^{-1}\partial\mathbf{E}/\partial\mathbf{Z}$, through Green's function perturbations to the zonal mean zonal wind acting on the zonal advection of eddies (Hassanzadeh and Kuang 2016). As shown in Eq. (5), this feedback matrix bridges the direct response in zonal wind to an arbitrary climate forcing and the full response with zonal advection feedback, which is analogous to the feedback parameter in the climate sensitivity framework. In this paper, we will focus on the application of this framework in CZL20 to an atmospheric model with a hydrological cycle and thermodynamic effects of water vapor.

b. *Overriding method for the zonal advection feedback*

This forcing–feedback framework was supported by examining the sensitivity of the westerly jet stream in a dry atmospheric dynamical core to a number of idealized mechanical and thermal forcings, using an overriding method for zonal mean zonal wind analogous to overriding SST for the sensitivity of surface temperature to greenhouse gas increases (CZL20). In this study, we will extend this overriding method to an aquaplanet model with moisture's impacts on radiation and convection such that we can quantify the contribution of zonal advection feedback to the zonal circulation responses to greenhouse gas increases with more realistic radiative and moist processes. More specifically, we prescribe the zonal-mean zonal wind used in the zonal advection of eddies in the overriding version of an atmosphere model by using the zonal

wind taken from the standard control simulation, while the zonal-mean zonal wind remains a predictive variable in the overriding model. This is implemented numerically by overriding the effects of anomalous zonal flow on the zonal advection of vorticity ζ, temperature T, and specific humidity Q as

$$\frac{D^{\mathrm{Ovrd}}\zeta}{Dt}=\frac{D\zeta}{Dt}+\frac{(\overline{u}^{\mathrm{Ovrd}}-\overline{u})}{a\cos\varphi}\frac{\partial\zeta}{\partial\lambda}, \tag{6}$$

$$\frac{D^{\mathrm{Ovrd}}T}{Dt}=\frac{DT}{Dt}+\frac{(\overline{u}^{\mathrm{Ovrd}}-\overline{u})}{a\cos\varphi}\frac{\partial T}{\partial\lambda}, \quad \text{and} \tag{7}$$

$$\frac{D^{\mathrm{Ovrd}}Q}{Dt}=\frac{DQ}{Dt}+\frac{(\overline{u}^{\mathrm{Ovrd}}-\overline{u})}{a\cos\varphi}\frac{\partial Q}{\partial\lambda}, \tag{8}$$

where λ is longitude, φ is latitude, and a is Earth's radius; D/Dt denotes the total derivative of vorticity, temperature, or moisture. Overbars denote zonal means. As such, the zonal mean zonal wind in the zonal advection of eddies u is replaced by u^{Ovrd}, and the model-generated zonal mean zonal wind cannot directly influence the eddies by zonal advection. In practice, u^{Ovrd} uses the 6-hourly zonal-mean zonal wind from the standard control run. The 6-hourly data are linearly interpolated in time within the 6-hourly interval to provide a continuously varying time series as input for the overriding model.

It is readily seen that the above overriding formulation does not directly modify the zonal mean of the nth power of vorticity, temperature, and specific humidity, that is, $D^{\mathrm{Ovrd}}\overline{\zeta}^n/Dt=D\overline{\zeta}^n/Dt$, $D^{\mathrm{Ovrd}}\overline{T}^n/Dt=D\overline{T}^n/Dt$, and $D^{\mathrm{Ovrd}}\overline{Q}^n/Dt=D\overline{Q}^n/Dt$. These relations ensure global conservations (e.g., energy or enstrophy) in the overriding model, although the added terms may introduce local sources or sinks owing to the difference between prescribed $\overline{u}^{\mathrm{Ovrd}}$ and model-generated $\overline{u}$. Physically speaking, this overriding method can be thought of as modifying the zonal propagation speed of eddies by $\overline{u}^{\mathrm{Ovrd}}-\overline{u}$, similar to a Doppler shift. It is important to note that the zonal advection feedback is much stricter than generic eddy feedback mechanisms discussed in the literature, as for instance it may exclude the impact of changes in static stability on a zonal jet. Hassanzadeh and Kuang (2016) directly analyzed the eddy feedback from the changes in temperature in a dry atmospheric dynamical core, but it is unclear how their analysis could be extended to models with more realistic radiative and moist processes.

More generally, the overriding method may be written as

$$\frac{D^{\mathrm{Ovrd}}\chi}{Dt}=\frac{D\chi}{Dt}+\frac{(\overline{u}^{\mathrm{Ovrd}}-\overline{u})}{a\cos\varphi}\frac{\partial\chi}{\partial\lambda}. \tag{9}$$

Here in accordance with Eqs. (6)–(8), χ approximately denotes potential temperature, water vapor, and potential vorticity (by a combination of vorticity and temperature), respectively. This indicates that the zonal advection feedback represents the influence of zonal wind on quasi-conservative tracers through the speed of zonal advection. Since the added terms will not directly alter the zonal means of dynamical fields ($D^{\mathrm{Ovrd}}\overline{\chi}/Dt=D\overline{\chi}/Dt$), the zonal advection feedback indeed represents an eddy feedback mechanism, and thus one can use the conventional diagnostics of eddy–zonal flow interactions to understand the underlying mechanisms. Additionally, while only zonal mean zonal wind is considered for feedback, temperature will vary consistently with the changes in zonal wind through the thermal wind balance, and the changes in mean meridional circulation are still constrained by the angular momentum budget.

In this study, we will not directly compute the feedback matrix as in CZL20 but will focus on the distinctions between the direct response and zonal advection feedback in terms of temperature, zonal wind, energy, and hydrological cycles under greenhouse gas increases. The direct response is expected to capture the thermal structure of the atmosphere under greenhouse gas increases, whereas the feedback component is thought to reflect the dynamical processes due to changes in zonal advecting speed of synoptic weather systems.

3. Numerical model and experiments

a. Experiment design

The numerical model used in this study is an idealized moist general circulation model (GCM) described in Clark et al. (2018), based on the GFDL spectral atmospheric dynamical core. The model uses a simplified Betts–Miller parameterization of convection (Frierson 2007). When water vapor condenses through large-scale atmospheric processes or the convection scheme, condensational heat is released instantaneously, and condensed water leaves the atmosphere as rainfall (Merlis et al. 2013). Because condensed water falls out as precipitation immediately, there are no parameterizations of clouds or no cloud radiative effects in the model. The model is coupled to a slab ocean as the boundary condition with a depth of 1 m for fast equilibration. Furthermore, a gray-atmosphere scheme with a comprehensive radiative transfer is employed to allow the water vapor–radiation feedback (Paynter and Ramaswamy 2014). The simulations are run with zero obliquity and eccentricity to remove any seasonal cycle in solar insolation (i.e., the perpetual equinox condition). The carbon dioxide concentration is varied over a broad range of values (to be described below), while the mixing ratios of other important well-mixed greenhouse gases, such as methane and nitrous oxide, are prescribed to present-day values. A hemispherically symmetric, latitudinally and vertically varying profile of ozone is prescribed to the radiation scheme as in Blackburn et al. (2013).

To assess the contributions of zonal advection feedback to the zonal circulation response to CO_2 changes, we have conducted five simulations with different values of carbon dioxide concentration and five corresponding overriding simulations, respectively. The standard control simulation is performed with the preindustrial (PI) CO_2 concentration (i.e., 280 ppm, referred to as the PI_Full run hereafter). The other four full runs use the quarter, half, double, and quadruple of the preindustrial CO_2 value (referred to as 1/4 × CO_2_Full, 1/2 × CO_2_Full, 2 × CO_2_Full, and 4 × CO_2_Full runs, respectively, hereafter). In the corresponding five overriding simulations, the settings are the same as the quartering, halving, PI, doubling, and quadrupling CO_2 experiments, respectively, except that the overriding approach is applied with the zonal wind used for zonal advection held the same as those from PI_Full run (referred to as 1/4 × CO_2_Ovrd, 1/2 × CO_2_Ovrd, PI_Ovrd,

TABLE 1. Description of model experiments.

No.	Experiment name	Experiment description
1	1/4 × CO_2_Full	1/4 of PI CO_2 value
2	1/2 × CO_2_Full	1/2 of PI CO_2 value
3	PI	PI CO_2 (280 ppm)
4	2 × CO_2_Full	2 times of PI CO_2 value
5	4 × CO_2_Full	4 times of PI CO_2 value
6	1/4 × CO_2_Ovrd	Same as 1, but using zonal wind from PI for zonal advection
7	1/2 × CO_2_Ovrd	Same as 2, but using zonal wind from PI for zonal advection
8	PI_Ovrd	Same as 3, but using zonal wind from PI for zonal advection
9	2 × CO_2_Ovrd	Same as 4, but using zonal wind from PI for zonal advection
10	4 × CO_2_Ovrd	Same as 5, but using zonal wind from PI for zonal advection
11	PI_ZA_4 × CO_2	Same as 8, but using zonal wind from 5 for zonal advection

2 × CO_2_Ovrd and 4 × CO_2_Ovrd run, respectively). All the simulations are listed in Table 1. Each experiment was run for 30 model years, with the first 6 years discarded as spinup. The time mean quantities in the PI_Full or PI_Ovrd run are regarded as the reference state. The response to CO_2 changes in the full simulations is obtained as the deviation from the PI_Full run and named as the full response. Similarly, the response in the overriding simulations is computed as the deviation from the PI_Ovrd run. Since the zonal wind used in the zonal advection of the overriding runs is held unchanged from PI_Full, the response in overriding runs represents the direct response of zonal circulation to CO_2 changes. The full response minus its corresponding direct response describes the circulation changes due to the zonal advection feedback [Eq. (5)]. We will evaluate the linearity between the direct response and the zonal advection feedback in the next section.

b. *Evaluation of the overriding method*

Before we conduct the feedback analysis for the model over a range of CO_2 concentrations, it is important to verify that the overriding method would not significantly alter the climatology and unforced variability of the control simulation. We first present the time mean and the leading empirical orthogonal function (EOF1) of daily zonal mean zonal wind in the PI_Full run and PI_Ovrd run (Figs. 2a,b). The spatial patterns of zonal mean zonal wind climatology in these two runs are almost the same. The leading mode of variability (i.e., the annular mode) in the standard control simulation, PI_Full run, features an equivalent barotropic pattern that represents the north–south vacillation of the jet stream (Fig. 2a). This pattern is well reproduced in the PI_Ovrd run (Fig. 2b). The daily temporal evolution of zonal mean zonal wind at 200 hPa and its jet latitude in the full run and overriding run are shown in Figs. 2c–e. The zonal jet variation is similar in the two runs over the time scales of longer than 10 days, with slightly less meridional vacillation in the overriding run. The low-frequency variability of midlatitude water vapor is also similar between the two control runs (Fig. 2f). Given the chaotic nature of the atmosphere, the similarity in low-frequency variability between the PI_Full and PI_Ovrd runs can be only attributed to the eddy forcing that is largely organized by the same anomalous advecting zonal wind used for zonal advection. This comparison explicitly demonstrates that the zonal mean zonal wind used in the zonal advection of eddies plays a critical role in the spatial structure and low-frequency variability of a zonal jet. The differences between the standard and overriding runs are induced by the inconsistency on short time scales in the overriding run between the model-generated zonal wind and the prescribed zonal mean zonal wind for the advection of vorticity, temperature, and specific humidity, but these differences become minor on long time scales. This is consistent with previous findings on the annular mode feedback that eddies are stochastic on short time scales but are organized by the zonal jet on long time scales (e.g., Lorenz and Hartmann 2001; Ring and Plumb 2008; Chen and Plumb 2009). Thus, the combination of the standard and overriding runs can be used to study the jet sensitivity to climate forcing.

We have also compared the global mean surface temperature and radiative balance at the top of atmosphere (TOA) for the standard and overriding runs with a wide range of CO_2 concentrations (Fig. 3). The global mean surface temperature rises almost linearly with the exponential increase of CO_2 concentration (Fig. 3a), in line with many previous studies and IPCC reports (IPCC 2013). Since there is no cloud or sea ice in this idealized aquaplanet model, the primary radiative feedbacks are Planck and water vapor feedbacks. The warming planet emits more outgoing longwave radiation at TOA, which is balanced by the changes in shortwave radiation absorption due to the enhanced water vapor (Figs. 3b,c). The differences in global mean surface temperature and TOA radiation balance are negligible between the full and overriding runs as compared to their responses to CO_2 perturbations, further corroborating that the overriding method does not significantly influence the global energy balance.

As demonstrated in section 2, the full response of the zonal mean circulation can be decomposed into two components, the direct response and the zonal advection feedback, and thus it is necessary to evaluate the linearity between these two components in the model simulations. To achieve this aim, we conducted an additional overriding experiment to directly isolate the effect of zonal advection on eddies due to changes in zonal mean zonal wind. In this additional overriding simulation, CO_2 is kept at PI levels while u^{Ovrd} or zonal advection is taken from the 4 × CO_2 full simulation (named as PI_ZA_4 × CO_2 run and listed in the Table 1). The difference between the PI_ZA_4 × CO_2 run and the PI_Ovrd run is the effect of zonal

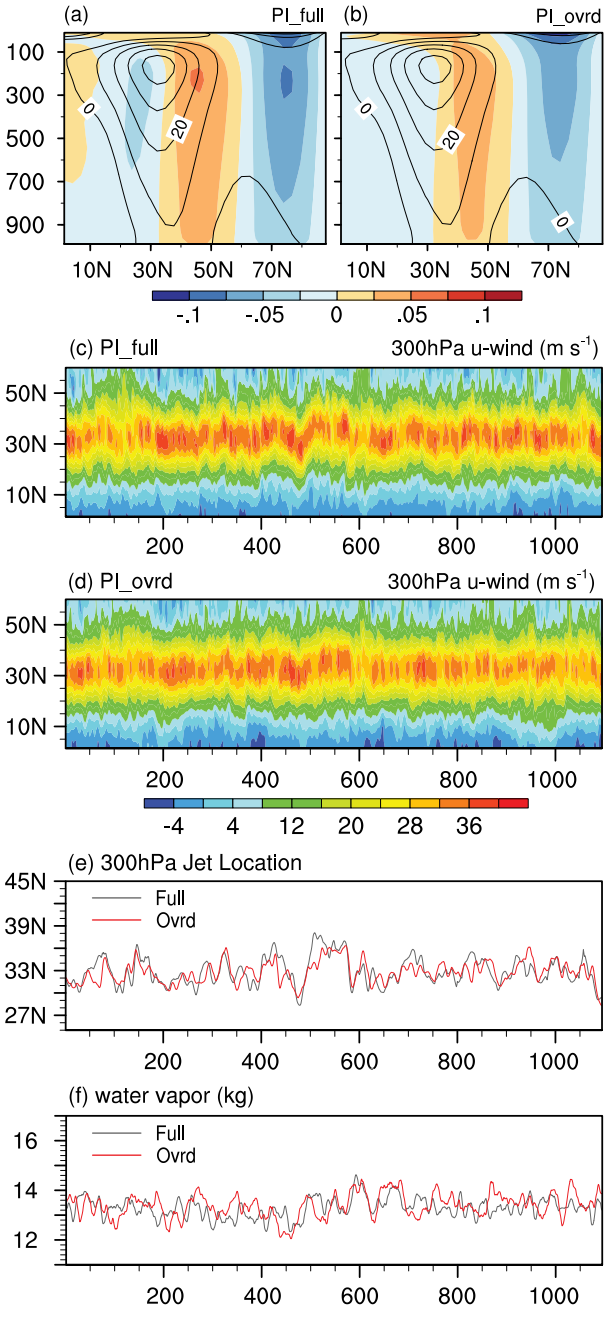

FIG. 2. Comparison of zonal mean zonal wind between the full and overriding PI simulations. (a),(b) Leading EOF (EOF1) of daily zonal mean zonal wind over the Northern Hemisphere in the PI_Full and PI_Ovrd simulations. Contours in (a) and (b) are the climatological means of zonal mean zonal wind. (c),(d) Daily evolutions of 300-hPa zonal mean zonal wind over the Northern Hemisphere midlatitudes in the PI_Full and PI_Ovrd simulations. (e) Daily time series of 300-hPa jet latitude in the PI_Full and PI_Ovrd simulations. (f) Daily time series of water vapor in the troposphere (below 300 hPa) over the midlatitude (30°–50°N). A 9-day running average is applied in time in (e) and (f), and only a 3-yr period is shown for better illustration.

advection on eddies due to changes in zonal mean zonal wind, in the absence of any direct response to CO_2 changes. The sum of the direct response and zonal advection feedback can be used to assess the nonlinearity in the full response. Here we compare the sum of two components to the full response in Fig. 4 for the zonal-mean zonal wind at 100 and 925 hPa, respectively. There is some nonlinearity in the tropical upper troposphere, and this is expected from the nonlinear interaction between the Hadley cell and westerly jet (Lee and Kim 2003) and also discussed in CZL20. Nevertheless, the sum of two components is quantitatively close to the full response over the subtropics and midlatitudes (20°–55°N/S) where the westerly jet is located, indicating that the direct response and the zonal advection feedback are largely linearly additive, especially for the eddy-driven jet. Thus, in the following sections, the zonal advection feedback is indirectly taken as the difference between the full response and the direct response. This simplification greatly reduces the computational costs for the zonal advection feedback.

4. Contrasting the direct response to quadrupling CO_2 with zonal advection feedback

In this section, we will describe the characteristics of the atmospheric response to quadrupling CO_2 in the full simulations ($4 \times CO_2$_Full − PI_Full), the corresponding direct response in the overriding simulations ($4 \times CO_2$_Ovrd − PI_Ovrd), and their difference due to the zonal advection feedback. The results are approximately opposite in sign for the quartering CO_2 experiments ($1/4 \times CO_2$_Full and $1/4 \times CO_2$_Ovrd runs) and thus are not shown here.

Starting with atmospheric thermal structure, the full and overriding runs (Figs. 5a and 5c) display the well-known spatial patterns of the temperature response to an increase in CO_2, with elevated upper tropospheric warming in the tropics, lower tropospheric warming in the polar regions, and cooling in the stratosphere (e.g., Manabe and Wetherald 1967). The elevated warming in the tropical upper troposphere can be understood as the moist adiabatic lapse rate adjustment to surface warming in a moister atmosphere (e.g., Manabe and Wetherald 1967); the near-surface warming in the polar region is expected from a moist diffusive energy balance model (EBM) in a warming climate even without any surface albedo feedback (e.g., Merlis and Henry 2018). These tropospheric warming patterns can affect baroclinic instability (e.g., measured by the Eady growth rate) by increased static stability in the tropics and subtropics, decreased meridional temperature gradient in the lower troposphere, and increased meridional temperature gradient in the upper troposphere and lower stratosphere. Consistent with the temperature changes and thermal wind balance, the full and direct responses in zonal mean zonal wind are characterized by an upward and poleward shift in the westerly jet, with a large zonal acceleration near the tropopause (Figs. 5b and 5d).

The zonal advection feedback, obtained as the difference between the full and overriding runs, results from the influence of the direct response in zonal wind on the zonal advection of eddies, as described in section 2a. CZL20 found that the zonal wind acceleration near the tropopause in the direct response

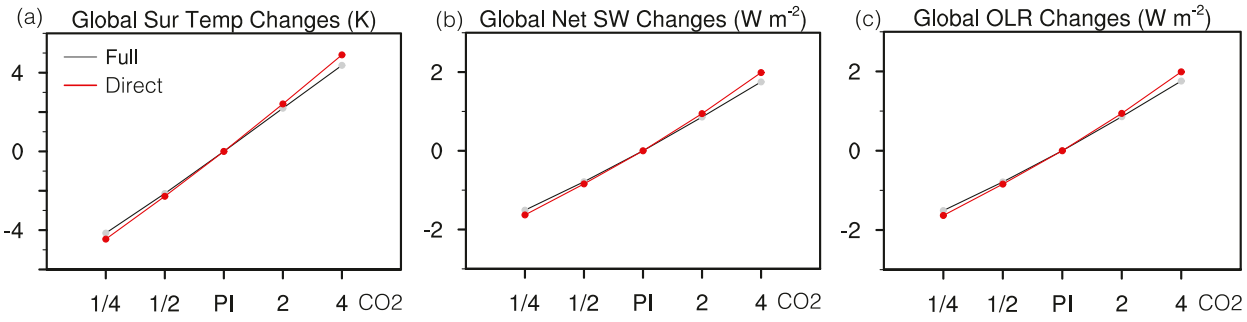

FIG. 3. Changes in (a) global mean surface temperature, (b) incoming shortwave radiation at TOA, and (c) outgoing longwave radiation (OLR) in response to CO_2 changes in the full (gray) and overriding (red) simulations. The horizontal axis shows the experiments with different CO_2 concentration listed in Table 1.

leads to an annular mode–like response in the zonal advection feedback. While the dry model in CZL20 is much simpler than the moist model used here, their feedback analysis supports the large zonal acceleration near the tropopause in the direct response in Fig. 5d leading to an annular mode–like feedback in Fig. 5f. Also, the temperature changes from the zonal advection feedback feature dynamically driven tropical warming and polar cooling in the stratosphere (Fig. 5e), consistent with the temperature pattern associated with a poleward jet shift (Fig. 3c of CZL20). Remarkably, while the direct jet shift in response to the CO_2 increase is comparable in magnitude with the poleward jet shift due to the zonal advection feedback and both fulfill the thermal wind balance, the signs of their corresponding temperature changes are different, implying distinct physical processes. The low stratospheric cold anomalies over the high latitudes and tropical warming can be thought of as a dynamical response in the lower branch of the Brewer–Dobson circulation to changes in the lower-stratospheric wave drag, which result from the changes in transient eddies that drive the jet changes. The tropospheric cooling in the extratropics is also associated with an increase in the jet strength through the thermal wind relation. And the subsequent changes in water vapor are likely to provide additional radiative feedback. The thermodynamic equation will reach a new balance from changes in both the dynamical effect and radiative effect.

Changes in zonal wind for the direct response and feedback are accompanied by distinct changes in mean meridional circulation and relative humidity. The full response to quadrupling CO_2 (Figs. 6a) shows a weaker Hadley cell, with an upward shift and poleward expansion in the Hadley cell and a poleward shift in the Ferrel cell. The weakening of the Hadley cell is larger in the overriding run than that in the full simulation (Fig. 6c), as the zonal advection feedback tends to strengthen the mean meridional circulation to counteract the direct response (Fig. 6e). The feedback also reinforces the Hadley cell expansion (Fig. 6e), consistent with the poleward shift of the westerly jet (Fig. 5f). These consistent changes between meridional circulation and zonal wind may be at least partly understood by the near-surface angular momentum budget, in which changes in the surface friction due to a poleward jet shift must be balanced by changes in the Coriolis force induced by the meridional circulation. Furthermore, previous studies have suggested that changes in the Hadley cell and westerly jet could lead to changes in relative humidity in the atmosphere (e.g., Wright et al. 2010), although thermodynamic changes alone may largely explain the changes to relative humidity and cloud fractions (e.g., Ming and Held 2018). The full response to quadrupling CO_2 (Fig. 6b) exhibits a horseshoe-shaped decrease in relative humidity in the tropical upper troposphere, subtropics, and extratropics, and an increase in the tropical midtroposphere and the stratosphere. The relative humidity changes in the troposphere can be explained by the poleward shift of mean meridional circulation (Fig. 6a). The relative humidity increase at the lower stratosphere can be attributed to the tropopause lifting due to greenhouse gas augment (Vallis et al. 2015), and to more water vapor entering the stratosphere through the tropical tropopause layer due to CO_2 increases (e.g., Dessler et al. 2013). With the suppression of zonal advection feedback, the subtropical decrease and lower stratospheric increase is weakened in the overriding run (Fig. 6d). By calculating the difference, we can see that the zonal advection feedback accounts for about half of the subtropical decrease and more than half of the lower stratospheric increase in relative humidity (Fig. 6f).

The above comparison between the direct response to quadrupling CO_2 and zonal advection feedback highlights two distinct mechanisms (i.e., direct thermodynamic effects versus changes in zonal mean advecting speed) in the atmospheric response to greenhouse gas increases: while both the direct response and feedback exhibit a poleward expansion of the Hadley cell and a poleward jet shift, the direct response displays a tropospheric warming pattern almost the same as the full response, but the feedback component shows very weak tropospheric cooling. This indicates that the direct response is predominantly an atmospheric thermodynamic response, but the feedback is due, by design, to the modulations of the westerly jet on the zonal advection of eddies. Therefore, we will further analyze the changes in meridional energy transport and hydrological cycle, in which the thermodynamic and zonal momentum processes are expected to be distinct from each other.

Figure 7 displays individual components of the response to quadrupling CO_2 for 100-hPa zonal-mean zonal wind (denoting the subtropical jet changes near the tropopause; see Fig. 5b), near-surface zonal wind, and meridional energy

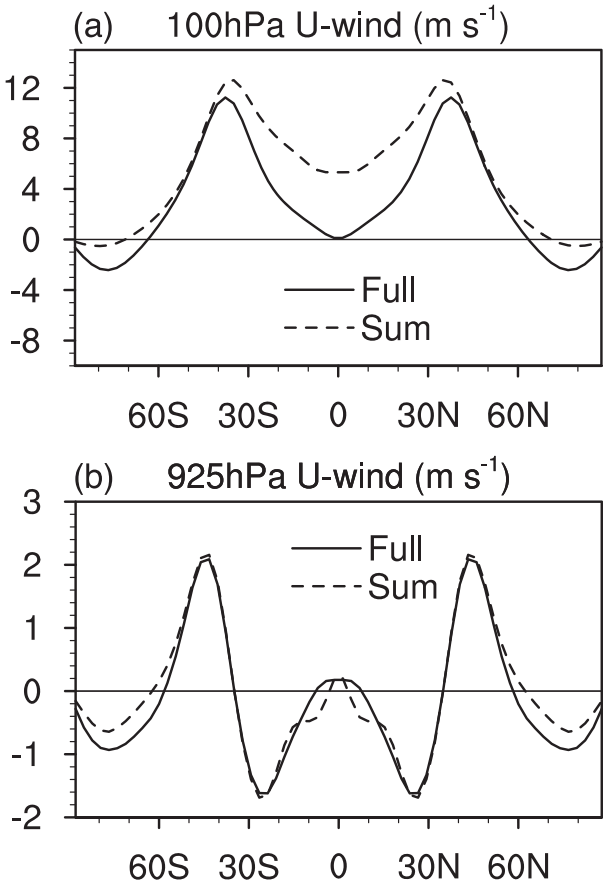

FIG. 4. Full response and the sum of the direct response and zonal advection feedback for the zonal mean zonal wind at (a) 100 and (b) 925 hPa with 4 × CO_2 forcing. The solid line denotes the full response directly calculated as 4 × CO_2 minus PI. The dashed line denotes the sum of the direction response (4 × CO_2_Ovrd − PI_Ovrd) and the zonal advection feedback (PI_ZA_4 × CO_2 − PI_Ovrd). Note that because the forcing is hemispherically symmetric, the average of two hemispheres is presented for climatological means, i.e., the two hemispheres in each subplot are identical (hereafter the same).

transport. The upper tropospheric jet maximum is located at 30°N/S in the PI_Full run (Fig. 7a, dashed gray line). The response to quadrupled CO_2 gives an increase in jet speed with more acceleration on the jet's poleward flank (black line); the contributions of the direct response and feedback are comparable for both the shift and intensification of the upper-level jet (Fig. 7a). Similar contributions of the direct response and feedback are found for the poleward shift of surface westerlies (Fig. 7c). The poleward shift in near-surface zonal winds is in agreement with the shift in the Hadley cell and Ferrel cell (Fig. 6). By contrast, the meridional energy transport in the full response is dominated by the direct response (Fig. 7e), as also implied by the global energy balance (Fig. 3); the feedback only weakens the poleward energy transport around 30°–40°N/S, where the largest zonal jet responses are located (Fig. 7e). These results suggest that changes in meridional energy transport under quadrupling CO_2 are dominated not by changes to mean meridional circulation, but by thermodynamic changes.

The contributions to changes in the hydrological cycle are presented in the forcing–feedback framework as well. Figure 7b shows the column-integrated water vapor in the atmosphere, in which the moisture increase under quadrupling CO_2 is due mostly to tropospheric warming in the direct response; the zonal advection feedback in fact produces a very weak moisture decrease in the subtropics likely owing to tropospheric cooling (Fig. 4e). The differences in temperature are also reflected in changes to precipitation minus evaporation ($P - E$), a measure of the global water vapor budget. Both the full and direct responses roughly show a drying effect in the subtropical regions where mean $P - E < 0$ and a wetting effect in the extratropics where mean $P - E > 0$ (Fig. 7f), a well-known thermodynamic mechanism for the hydrological cycle response to global warming (e.g., Chou and Neelin 2004; Held and Soden 2006). The direct response also shows significant deviations from a pure thermodynamic effect, in particular with a poleward shift in the edge of subtropical dry zone, where mean $P - E = 0$. The feedback, in contrast, contributes mostly to the subtropical decline in precipitation. Changes in tropical precipitation are largely cancelled between the direct response and feedback. Furthermore, similar to changes in $P - E$, the precipitation response in the full simulation displays an increase in the extratropics and a decrease in the subtropics, and thus the midlatitude rainbelt moves poleward along with the poleward shift in westerlies (Fig. 7d). Interestingly, the midlatitude increase in extratropical precipitation is dominated by the direct response (i.e., both an increase in atmospheric moisture and a dynamical circulation shift), but the decrease in subtropical precipitation is mainly caused by feedback.

In summary, the feedback analysis of the aquaplanet model under quadrupling CO_2 has identified an eddy feedback mechanism associated with changes in zonal mean advecting wind that resembles the feedback in the dry atmospheric dynamical core (CZL20). In comparison with the well-known thermodynamic response to a CO_2 increase, the zonal advection feedback exhibits a lower-stratospheric temperature pattern with tropical warming and polar cooling, and also explains nearly half of the changes to the eddy-driven jet shift and Hadley cell expansion and a large portion of the decline in subtropical precipitation.

5. Assessing the direct response to CO_2 changes versus feedback over a range of climates

Having characterized the influences of zonal advection feedback on global atmospheric circulation, we further quantify its contributions to the changes to the Hadley cell and westerly jet over a range of climates from quartering CO_2 to quadrupling CO_2. In particular, the boundary of the Hadley cell in the subtropics is defined as the latitude where the zonal mean meridional streamfunction at 500 hPa is zero. The magnitude of the Hadley cell is measured by the maximum of zonal mean meridional streamfunction at 500 hPa. The latitude and strength of the westerly jet are computed for the zonal mean zonal wind at both 100 hPa and near the surface.

The changes of the Hadley cell boundary and magnitude in the full and overriding runs are shown in Figs. 8a and 8b. The

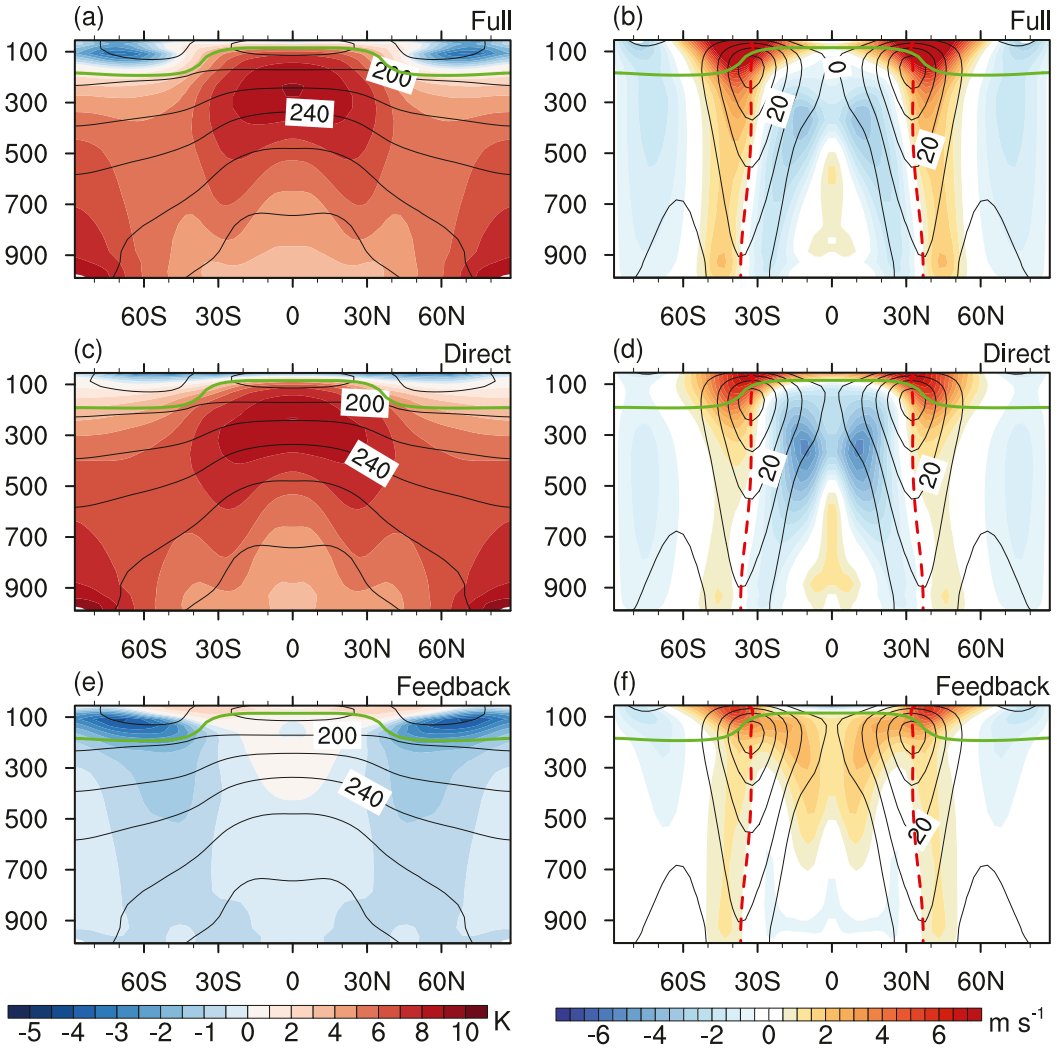

FIG. 5. Responses of (left) temperature and (right) zonal mean zonal wind to quadrupling CO_2. (a),(b) Responses in the 4 × CO_2_Full run (color shading) and the climatologies in the PI_Full run (contour). (c),(d) As in (a) and (b), but for the 4 × CO_2_Ovrd run. The contours in (c) and (d) denote the climatologies in the PI_Ovrd run. (e),(f) Zonal advection feedback (color shading) and the climatologies in the PI_Full run (contour). As introduced in section 2, the zonal advection feedback is calculated as the response in the full run minus the overriding run (hereafter the same). Red dashed lines in the right column indicate the latitude of the climatological jet. Green lines indicate the tropopause in their reference states, respectively.

Hadley cell expands and weakens roughly linearly with an exponential increase in CO_2. In particular, the Hadley cell edge extends poleward by about 2° in response to quadrupling CO_2 and shrinks equatorward by about 2° under quartering CO_2. This linearity is also found in the overriding runs, except for a smaller change in the Hadley cell width. On average, about 56% of the changes in the Hadley cell width are attributed to the direct response, and 44% is contributed by the zonal advection feedback. Furthermore, in contrast to the positive feedback to the Hadley cell expansion, the zonal advection feedback tends to offset the changes in the Hadley cell strength due to the direct response. While the direct response shows a linear decrease in the Hadley cell strength with an exponential growth in CO_2, the zonal advection feedback reduces this direct effect by about 29% (Fig. 8b).

Similar to the expansion of the Hadley cell, the latitude of both the upper-level jet and surface westerlies moves poleward approximately linearly with an exponential increase in CO_2 (Figs. 8c,e). The zonal advection feedback explains about one-third of the poleward shift in the upper-level jet at 100 hPa and half of the shift in surface westerlies. It is reasonable that eddy feedback contributes more to changes in surface westerlies than the upper-level jet, since surface westerlies are eddy-driven. In addition, the westerly wind speed increases with CO_2 concentration for both the upper troposphere and the surface (Figs. 8d,f). The zonal advection feedback explains most

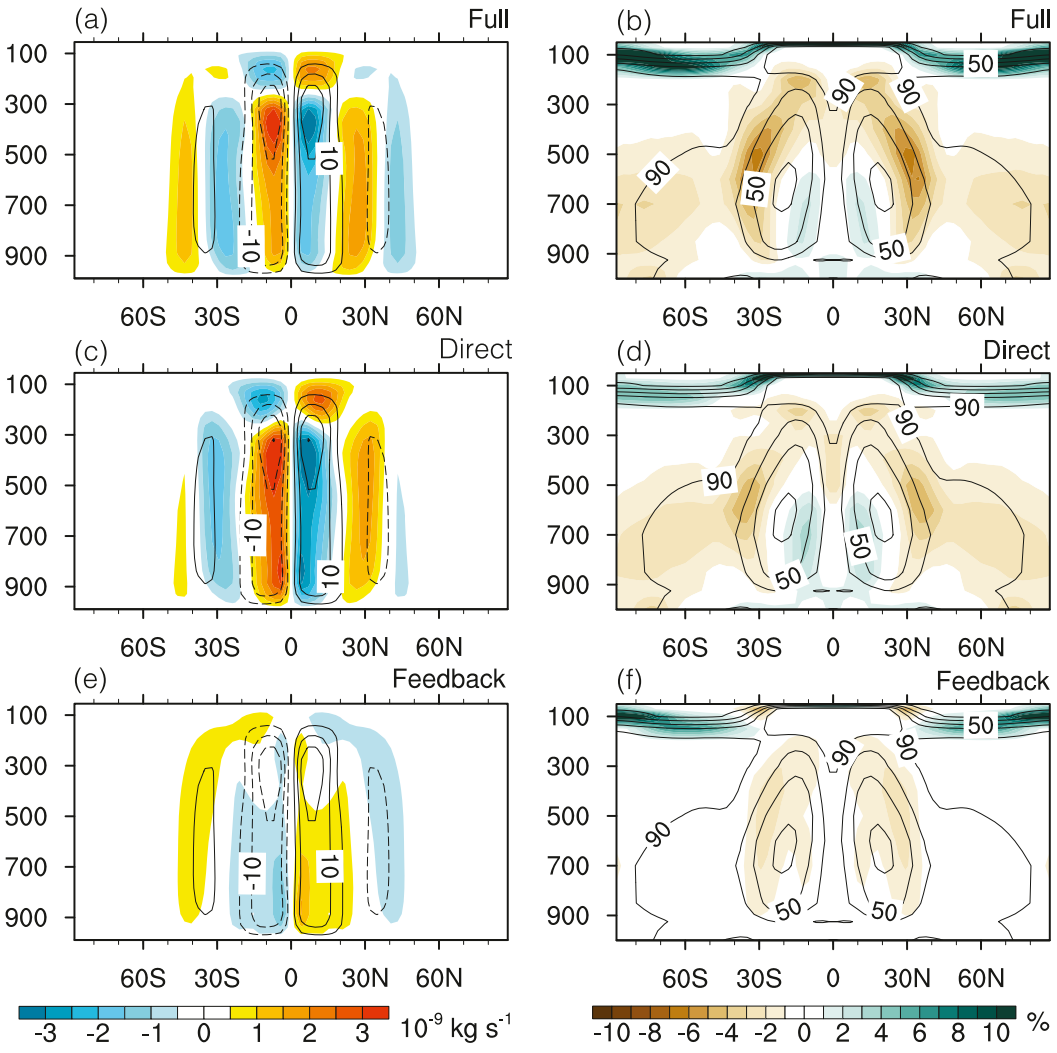

FIG. 6. Responses in (left) mean meridional circulation and (right) relative humidity to quadrupling CO_2. (a),(b) Responses in the 4 × CO_2_Full run (color shading) and the climatologies in the PI_Full run (contour). (c),(d) As in (a) and (b), but for the 4 × CO_2_Ovrd run. The contours in (c) and (d) denote the climatologies in the PI_Ovrd run. (e),(f) Zonal advection feedback (color shading) and the climatologies in the PI_Full run (contour).

of the increase in surface westerly strength (~70%), in contrast to nearly half of the jet strengthening at 100 hPa (~49%).

6. Eddy mechanisms in the forcing–feedback framework

While the forcing–feedback framework can quantify the relative contributions of the direct response versus zonal advection feedback to greenhouse gas increases, their underlying mechanisms are not explained. We now return to the conventional diagnosis of eddy–zonal flow interactions to understand their underlying mechanisms. We also reiterate that the direct response differs from a zonally symmetric response to given mechanical or thermal forcing discussed in the literature (e.g., Haynes et al. 1991; Kushner and Polvani 2004; Ring and Plumb 2008; Sun et al. 2013), as it includes the eddy forcing not in association with the zonal advection feedback. Previous studies using the initial-value large-ensemble approach have found different eddy characteristics before and after the westerly jet starts to shift poleward in response to climate forcing (Chen et al. 2013; Sun et al. 2013; Lu et al. 2014), and the direct response may be thought of the early stage of the temporal evolution of the zonal circulation in response to climate forcing.

In light of the Eady growth rate for baroclinic instability, an increase in static stability or a decrease in meridional temperature gradient would suppress eddy activities. We first examine the responses in static stability (N^2) and meridional temperature gradient (DT/DY). In the full response, the static stability is increased in the troposphere with quadrupling CO_2, especially over the tropics and subtropics (Fig. 9a), which can be explained from the moist adiabatic adjustment to surface warming (e.g., Manabe and Wetherald 1967). The static stability change is evident only in the direct response that is dominated by thermodynamic changes (Figs. 9c,e). The meridional temperature gradient is enhanced near the jet core in

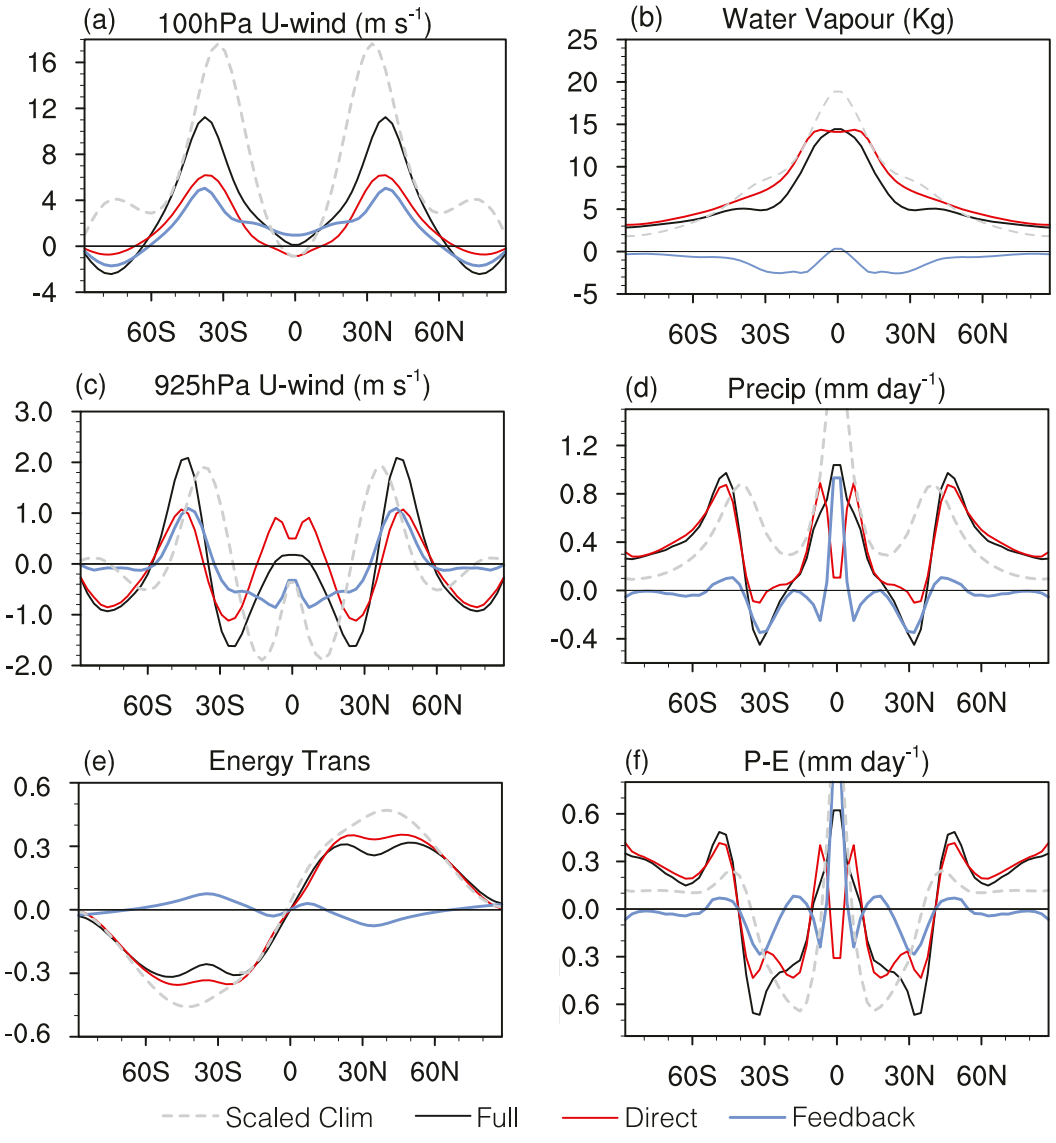

FIG. 7. Responses in (a) zonal mean zonal wind at 100 hPa, (b) column-integrated water vapor, (c) near-surface zonal wind, (d) precipitation, (e) meridional energy transport, and (f) precipitation minus evaporation ($P - E$) to quadrupling CO_2. The gray dashed lines indicate the climatological means scaled by a factor of 0.5 in (a) and (b); 0.2 in (c), (d), and (f); and 0.1 in (e). The solid black (red) line is the response in the full (overriding) simulation, and the solid blue line denotes the zonal advection feedback in each subplot.

both the full response and direct response (Figs. 9b,d), which largely results from the tropospheric warming and the downward tropopause slope with increasing latitude. The zonal advection feedback also contributes to the enhancement of meridional temperature gradient to the north of the jet core in the upper troposphere (Fig. 9f), but this is the result of a dynamical response to changes in the zonal mean advecting speed rather than a thermodynamic effect.

Figure 10 presents the eddy kinetic energy (EKE) climatology in the PI_Full run (contours) and the response in quadrupling CO_2 (colors) (Fig. 10a). The primary character in the EKE response is an upward and poleward shift of EKE, consistent with changes in comprehensive climate models under global warming (e.g., Lorenz and DeWeaver 2007; Wu et al. 2011). From the Lorenz energy cycle (Lorenz 1955), EKE gains energy from available potential energy by baroclinic conversion and loses energy to zonal mean kinetic energy through barotropic conversion. Remarkably, the direct response is characterized by an EKE increase over most regions (Fig. 10c), likely due to an increase in mean available potential energy from increased upper tropospheric meridional temperature gradient (Figs. 9b,d,a,c) (e.g., O'Gorman 2010), but the zonal advection feedback features a broad weakening in EKE (Fig. 10e), implicative of a negative feedback on EKE owing to the influence of the direct response in zonal wind. The upward and poleward shift of EKE in the full response results from the

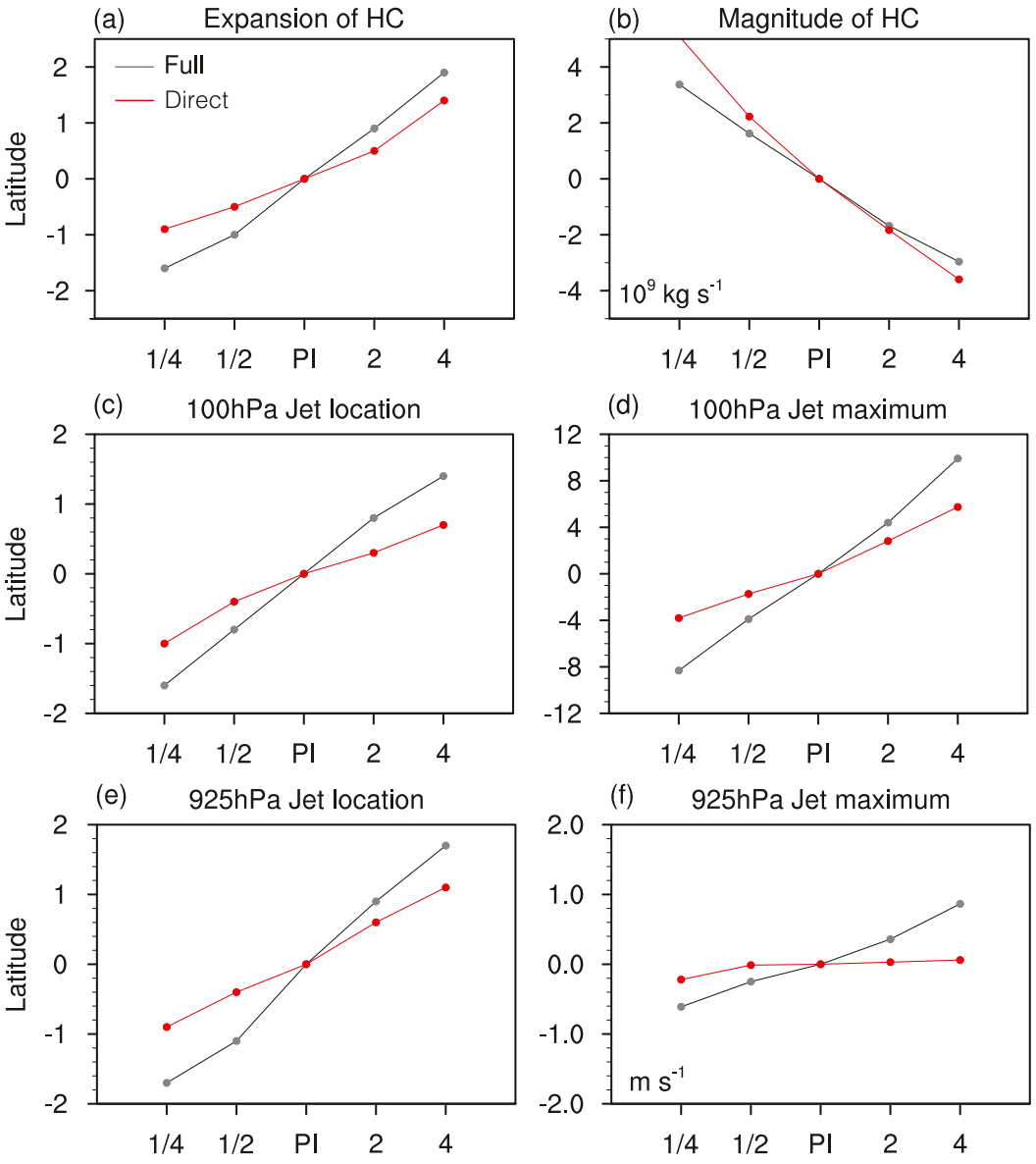

FIG. 8. Responses in the Hadley cell and westerly jet to changes in CO_2 in the full (gray) and overriding (red) runs: (a) the Hadley cell boundary, defined as the subtropical latitude where the zero contour of the meridional mass streamfunction at 500 hPa is located, (b) the magnitude of the Hadley cell, defined as the maximum of the meridional mass streamfunction at 500 hPa, (c) the location of the 100-hPa westerly jet, defined as the latitude where the maximum of the zonal mean zonal wind is located, (d) the maximum speed of the 100-hPa jet, (e) the location of the near-surface westerly jet, defined as the latitude where the maximum of the zonal mean zonal wind at 925 hPa is located, and (f) the maximum speed of the westerly jet at 925 hPa. The zonal mean variables are interpolated to 0.1° before the analysis.

cancellation of two opposite effects on EKE with some mismatch in their maximum locations.

How could the zonal advection feedback affect EKE? While the zonal advection feedback adds no extra term in the formulation of the Lorenz energy cycle, it could alter the phase speed of eddies and thus the vertical phase coupling in baroclinic waves, similar to the suppression of baroclinic instability in the atmosphere by a strong barotropic shear, known as the "barotropic governor" (James 1987). Using an initial-value large-ensemble approach, Chen et al. (2007) found the instantaneous response to a reduction in surface friction in a dry atmospheric dynamical core is a large reduction of EKE along with the development of a barotropic shear, which resembles the direct response in zonal wind to weakened surface friction (Fig. S7d of CZL20). This seems to corroborate the suppression of EKE in the aquaplanet model used here, which offsets the intensification in EKE due to enhanced mean available potential energy. Future analysis is warranted to better understand

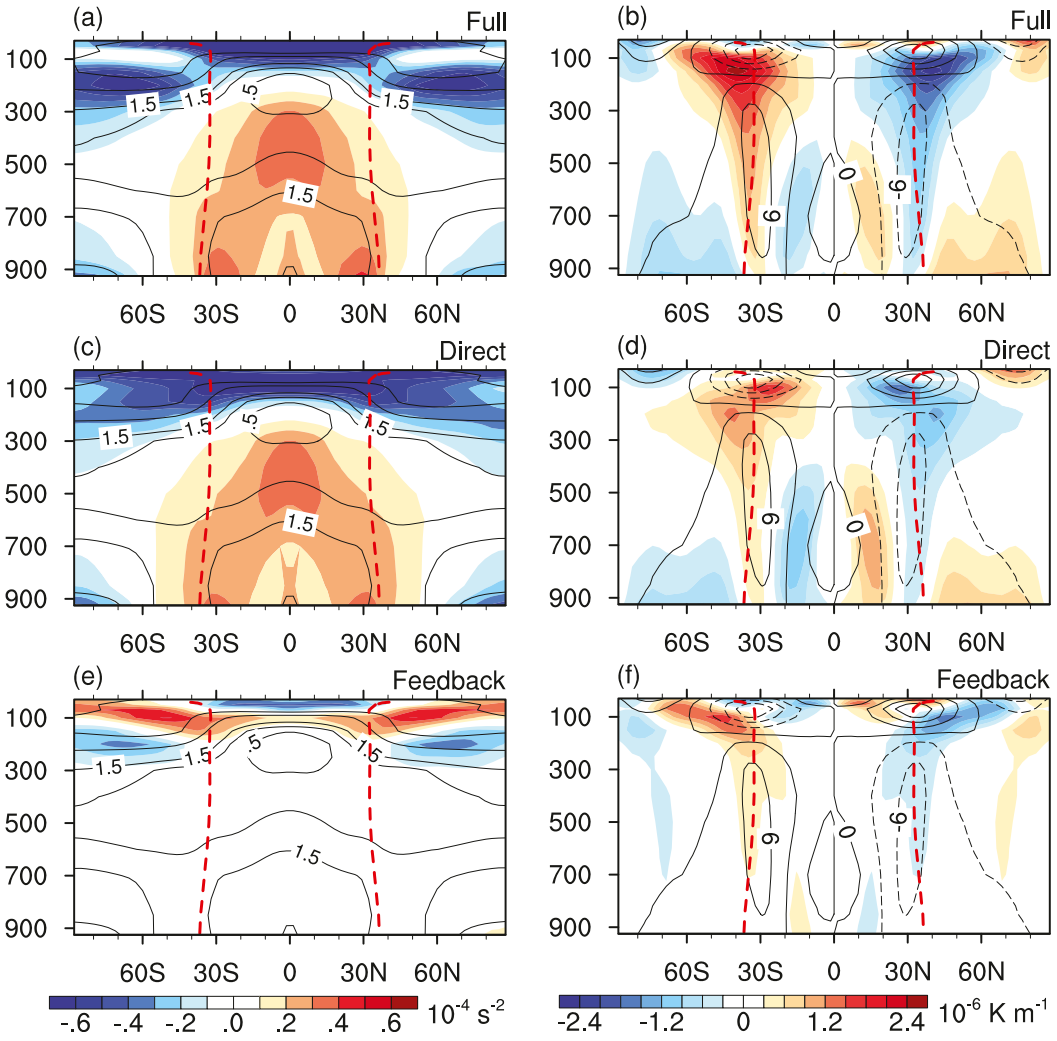

FIG. 9. Responses of (left) static stability (N^2) and (right) meridional temperature gradient (DT/DY) to quadrupling CO_2. (a),(b) Responses in the 4 × CO_2_Full run. The contours in (a) denote the climatology of static stability (the contours of 0.5, 1, 1.5, 3, 4.5, 6 × 10^{-4} s^{-2} are shown) in the PI run. The contours in (b) denote the climatology of latitudinal temperature gradient in the PI run (interval: 10^{-6} K m^{-1}). (c),(d) As in (a) and (b), but for the 4 × CO_2_Ovrd run. The contours in (c) and (d) denote the climatologies in the PI_Ovrd run. (e),(f) Zonal advection feedback and the climatologies in the PI run. Red dashed lines indicate the latitude of the climatological jet.

the relationship between zonal advection feedback and barotropic governor.

We further diagnose the eddy forcing exerting on the zonal flow using the Eliassen-Palm (EP) cross section (Edmon et al. 1980). The quasigeostrophic EP flux vector is written as $\mathbf{F} = (F_\varphi, F_P)$, with $F_\varphi = -a\cos\varphi\langle\overline{u^*v^*}\rangle$ and $F_P = af\cos\varphi(\langle\overline{v^*\theta^*}\rangle/\langle\theta\rangle_P)$, where f is the Coriolis parameter, u and v are zonal and meridional velocities, θ is potential temperature, angle brackets denote a zonal average, a superscript asterisk (*) denotes deviation from the zonal mean, and an overbar denotes a time average. The EP flux divergence is calculated as $[1/(a\cos\varphi)]\nabla\cdot\mathbf{F} = [1/(a\cos\varphi)]\{[1/(a\cos\varphi)][(\partial/\partial\varphi)(F_\varphi\cos\varphi)]+(\partial/\partial P)F_P\}$. The EP flux vector indicates the direction of wave propagation, and its convergence measures the wave forcing acting on the zonal wind. The meridional component of the EP flux is opposite in sign to the meridional eddy momentum flux (EMF), which indicates the direction of angular momentum transport by meridional wave propagation. The EMF divergence corresponds to the convergence of the meridional wave activity flux, where wave breaking tends to occur and cause the zonal wind deceleration. Similarly, the EMF convergence corresponds to the zonal wind acceleration, all other things being equal. From the perspective of the angular momentum budget, the upper-level EMF convergence corresponds to surface westerlies, and thus changes to EMF help explain changes in the eddy-driven jet.

The climatological mean EP fluxes are typically associated with baroclinic wave generation in the lower troposphere and upward propagation to the upper troposphere (Edmon et al. 1980). The subsequent equatorward wave propagation in the

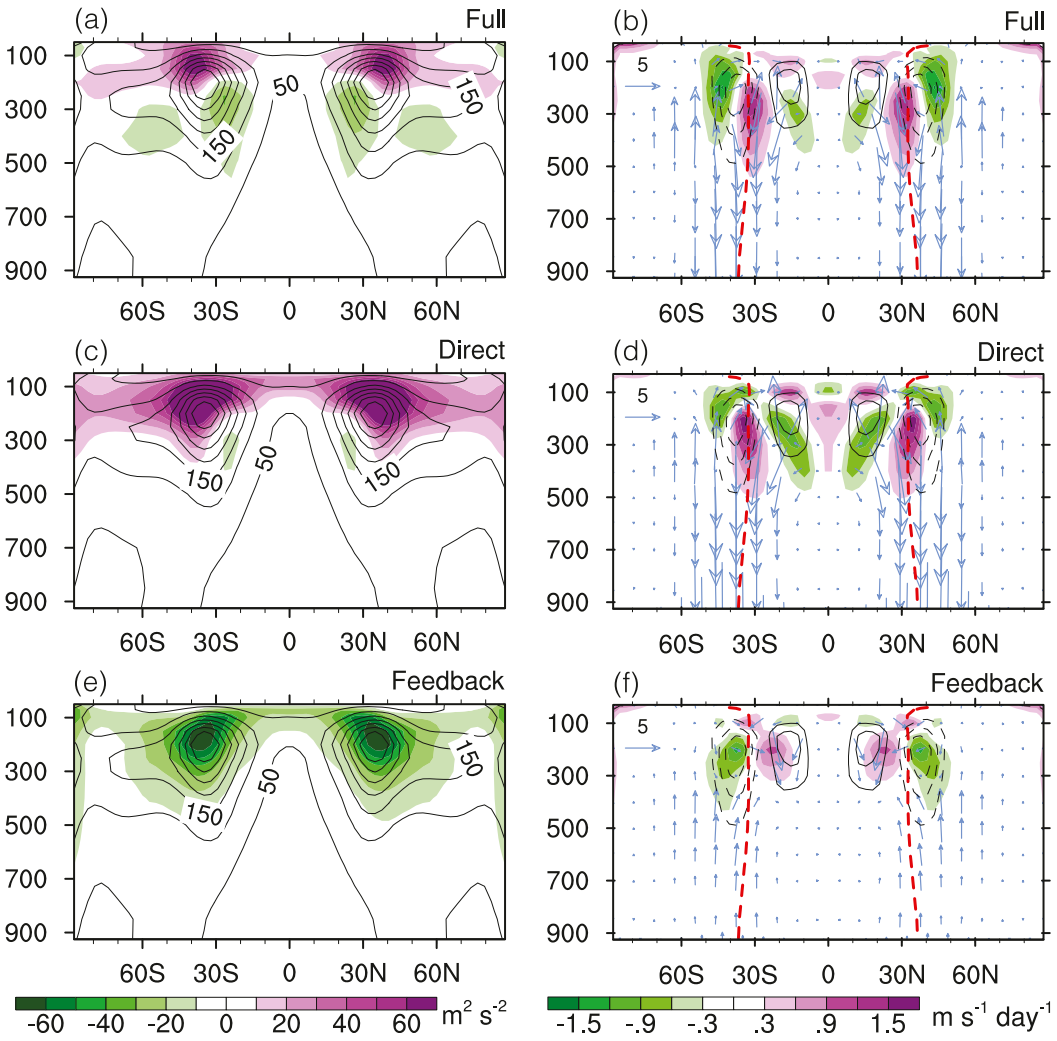

FIG. 10. Responses of (left) eddy kinetic energy and (right) eddy momentum flux divergence (color shading) and EP flux vector (vector) to quadrupling CO_2. (a),(b) Responses in the 4 × CO_2_Full run. The contours in (a) denote the climatology of eddy kinetic energy in the PI run. The contours in (b) denote the climatology of eddy momentum divergence in the PI run (interval: 1.5 m s^{-1} day^{-1}). The zero contour is omitted, and the negative values are dashed in (b). (c),(d) As in (a) and (b), but for the 4 × CO_2_Ovrd run. The contours in (c) and (d) denote the climatologies in the PI_Ovrd run. (e),(f) Zonal advection feedback and the climatologies in the PI_Full run. Red dashed lines indicate the latitude of the climatological jet.

upper troposphere corresponds to the EMF divergence in the subtropics and convergence in the midlatitudes (solid and dashed black lines in Fig. 10b, respectively). Figure 9b shows the full responses in the EP flux (vector) and EMF divergence (color) in the quadrupling CO_2 scenario. There are predominantly downward anomalies in the EP flux beneath the jet core, implicative of less baroclinic waves propagating into the upper troposphere in response to a CO_2 increase, likely due to the decreased lower tropospheric baroclinicity from increased subtropical static stability or decreased lower tropospheric meridional temperature gradient (see Figs. 9a,b). Thus, the EMF divergence displays an anomalous triple pattern, with a positive anomaly just below the jet core and negative anomalies on the jet's two flanks. Compared with the climatological EMF pattern, this indicates less wave-driven deceleration on the jet's equator flank (green shading and solid black lines), and a poleward shift in the midlatitude wave-driven acceleration (purple and green shading and dashed black lines).

Notably, the direct response gives an anomalous tripole pattern in EMF divergence similar to the full response, with less EMF convergence on the jet's poleward flank (Fig. 10d). This seems to be consistent with the mechanism that the increased subtropical static stability reduces the baroclinic instability there and moves the Hadley cell boundary and eddy-driven jet poleward (Held 2000). It also appears to resemble the eddy forcing in the early stage of the evolution in response to uniform SST warming using an initial-value large-ensemble approach (Fig. 10c of Chen et al. 2013). In contrast, the zonal

advection feedback, obtained from the difference of the full and direct responses, presents a salient dipole pattern, with an EMF divergence anomaly on the equatorward flank of the jet core and a convergence anomaly on the poleward flank (Fig. 10f). This dipole pattern about the jet core is similar to the EMF divergence associated with the annular mode variability (e.g., Lorenz and Hartmann 2001), in accordance with the importance of zonal advection feedback for the unforced annular mode variability in the control simulations (Fig. 2). Again, additional work is needed to understand the underlying eddy–mean flow interactions in the forcing–feedback framework.

The perspective of eddy–mean flow interactions is summarized as follows. The direct response to an increase in CO_2 displays a reduction in upward wave propagation and a poleward shift of midlatitude EMF convergence in association with a decrease in subtropical baroclinic instability. The zonal advection feedback, in contrast, features a dipole pattern in EMF that further shifts and strengthens midlatitude EMF convergence, which is, by design, caused by the large zonal wind increase in the upper troposphere and lower stratosphere seen in the direct response. Following the angular momentum budget, these changes in EMF, in turn, would lead to the poleward shift and strengthening of surface westerlies (Fig. 8c). Interestingly, while the direct response produces an increase in EKE, likely due to the increase in upper tropospheric meridional temperature gradient against the increase in subtropical static stability (Figs. 9c,d), the feedback weakens EKE, and this may be related to the suppression of EKE by barotropic shear, known as the barotropic governor (James 1987).

7. Conclusions and discussion

We have presented a new analysis of the atmospheric circulation response to greenhouse gas increases in an aquaplanet atmospheric model, using a recently developed forcing–feedback framework by CZL20. This framework focuses on the zonal advection feedback of zonal mean zonal wind (i.e., the effects of the zonal mean zonal wind on the zonal advection of vorticity, temperature, and moisture). Thus, the circulation response to a CO_2 increase is divided into two components: 1) the direct zonal wind response by holding the zonal mean zonal wind exerting on the zonal advection of eddies undisturbed, and 2) additional feedback induced by the direct response in zonal wind (Fig. 1).

Several well-known characteristics of atmospheric changes in a warming climate are examined with and without the zonal advection feedback, such as changes to the Hadley cell, midlatitude jets, storm tracks, and precipitation. It is found that while the direct response in temperature displays the well-known tropospheric warming pattern to an increase in CO_2 almost identical to the full simulation, the zonal advection feedback exhibits a weak lower-stratospheric temperature pattern with tropical warming and polar cooling, similar to that found in the dry atmospheric dynamical core (CZL20). Given that the aquaplanet model includes the radiative and convective effects of moisture, this work extends the analysis in a dry atmospheric dynamical core in CZL20 to more realistic radiative and moist processes for the atmospheric response to greenhouse gas increases. When the CO_2 concentration is varied exponentially from a quarter to quadruple the preindustrial concentration, the zonal advection feedback accounts for nearly half of the changes to the eddy-driven jet shift and Hadley cell expansion, with a large portion of the decline in subtropical precipitation. This demonstrates that the zonal advection feedback, albeit involving little surface warming, plays an important role in the circulation response to climate warming.

The forcing–feedback framework highlights the distinction of zonal mean advecting winds from the thermodynamic effects in the atmospheric response to greenhouse gas increases. To the best of our knowledge, it is the first analysis that attempts to quantify the relative contributions of the direct thermodynamic response to greenhouse gas increases and the feedback due to changes in zonal mean advecting winds. On one hand, the direct response is characterized by a reduction in upward wave propagation and a poleward shift of midlatitude EMF convergence. This appears to support the mechanism that the increased subtropical static stability reduces the baroclinic instability there and moves the Hadley cell boundary and eddy-driven jet poleward (Held 2000). On the other hand, the zonal advection feedback features a dipole pattern in EMF that further shifts and strengthens midlatitude EMF convergence, caused by the large zonal wind increase in the upper troposphere and lower stratosphere seen in the direct zonal wind response. This is corroborated by the feedback analysis with diverse thermal and mechanical forcings in CZL20. Interestingly, the direct response produces an increase in EKE, likely due to increased upper-level baroclinicity against decreased lower-level baroclinicity (Fig. 9) (e.g., O'Gorman 2010). The zonal advection feedback weakens EKE, which may be related to the suppression of EKE by barotropic shear, known as the barotropic governor (James 1987).

It is noteworthy that we have separated the eddy feedback due to the changes in static stability from the eddy feedback due to the changes in zonal mean advecting winds. This is because the increase in static stability under climate warming is much larger than the variation in static stability associated with the unforced annular mode variability. This separation may also help us better understand the differences in the circulation response to greenhouse gas increases versus the Antarctic ozone hole, as the latter displays a small change in subtropical static stability [see the review by Thompson et al. (2011)]. More specifically, the positive phase of the annular mode is characterized by a poleward shift in eddy-driven jet with a dipolar structure in eddy momentum flux convergence about the eddy-driven jet (Lorenz and Hartmann 2001). The eddy feedback from the zonal advection feedback (Fig. 10f) is largely consistent with the eddy forcing pattern associated with the unforced jet variability. In contrast, the increase in static stability under climate warming is evident only in the direct response (see Fig. 9), and the eddy feedback in the direct response (Fig. 10d) exhibits a tripolar structure in eddy momentum flux convergence about the eddy-driven jet. This suggests that the eddy feedback from the changes in static stability is distinct from the unforced annular mode variability or the zonal advection feedback.

This analysis has explicitly separated the contributions of atmospheric thermodynamic changes and zonal wind feedback to the circulation changes under climate warming in an aquaplanet atmospheric model with relatively realistic moist and radiative processes. However, care must be taken in generalizing our results to realistic climate projections. For example, there is no cloud radiative effect in this aquaplanet model configuration (see section 3a), while the cloud radiative effect, especially the shortwave radiation, could significantly contribute to the Hadley cell expansion and jet shift despite the cloud radiative feedback is model dependent (e.g., Ceppi and Hartmann 2016). Stationary waves, absent in the aquaplanet model, may also modulate the circulation response to climate warming, especially at the regional scales. The dynamics of the zonal advection feedback also warrants further investigation. For example, how does the feedback control the unforced variability of the zonal jet and eddy kinetic energy? This would provide new insights into the fundamental dynamics of annular modes and the suppression of barotropic shears on EKE.

Acknowledgments. We thank Dr. Yu Nie in CMA for helpful discussion. We would like to acknowledge high-performance computing support from Cheyenne (doi:10.5065/D6RX99HX) provided by CISL/NCAR, sponsored by the NSF. P.Z. and G.C. were funded by the NSF (AGS-1742178 and AGS-1832842).

REFERENCES

Barnes, E. A., and L. Polvani, 2013: Response of the midlatitude jets, and of their variability, to increased greenhouse gases in the CMIP5 models. *J. Climate*, **26**, 7117–7135, https://doi.org/10.1175/JCLI-D-12-00536.1.

Birner, T., 2010: Recent widening of the tropical belt from global tropopause statistics: Sensitivities. *J. Geophys. Res. Atmos.*, **115**, D23109, https://doi.org/10.1029/2010JD014664.

Blackburn, M., and Coauthors, 2013: The Aqua-Planet Experiment (APE): CONTROL SST simulation. *J. Meteor. Soc. Japan*, **91A**, 17–56, https://doi.org/10.2151/jmsj.2013-A02.

Ceppi, P., and D. L. Hartmann, 2013: On the speed of the eddy-driven jet and the width of the Hadley cell in the Southern Hemisphere. *J. Climate*, **26**, 3450–3465, https://doi.org/10.1175/JCLI-D-12-00414.1.

——, and ——, 2016: Clouds and the atmospheric circulation response to warming. *J. Climate*, **29**, 783–799, https://doi.org/10.1175/JCLI-D-15-0394.1.

Chang, E. K. M., Y. Guo, and X. Xia, 2012: CMIP5 multimodel ensemble projection of storm track change under global warming. *J. Geophys. Res. Atmos.*, **117**, D23118, https://doi.org/10.1029/2012JD018578.

Chemke, R., and L. M. Polvani, 2020: Linking midlatitudes eddy heat flux trends and polar amplification. *npj Climate Atmos. Sci.*, **3**, 8, https://doi.org/10.1038/s41612-020-0111-7.

Chen, G., and R. A. Plumb, 2009: Quantifying the eddy feedback and the persistence of the zonal index in an idealized atmospheric model. *J. Atmos. Sci.*, **66**, 3707–3720, https://doi.org/10.1175/2009JAS3165.1.

——, I. M. Held, and W. A. Robinson, 2007: Sensitivity of the latitude of the surface westerlies to surface friction. *J. Atmos. Sci.*, **64**, 2899–2915, https://doi.org/10.1175/JAS3995.1.

——, J. Lu, and D. M. W. Frierson, 2008: Phase speed spectra and the latitude of surface westerlies: Interannual variability and global warming trend. *J. Climate*, **21**, 5942–5959, https://doi.org/10.1175/2008JCLI2306.1.

——, ——, and L. Sun, 2013: Delineating the eddy–zonal flow interaction in the atmospheric circulation response to climate forcing: Uniform SST warming in an idealized aquaplanet model. *J. Atmos. Sci.*, **70**, 2214–2233, https://doi.org/10.1175/JAS-D-12-0248.1.

——, P. Zhang, and J. Lu, 2020: Sensitivity of the latitude of the westerly jet stream to climate forcing. *Geophys. Res. Lett.*, **47**, e2019GL086563, https://doi.org/10.1029/2019GL086563.

Chou, C., and J. D. Neelin, 2004: Mechanisms of global warming impacts on regional tropical precipitation. *J. Climate*, **17**, 2688–2701, https://doi.org/10.1175/1520-0442(2004)017<2688:MOGWIO>2.0.CO;2.

Clark, S. K., Y. Ming, I. M. Held, and P. J. Phillipps, 2018: The role of the water vapor feedback in the ITCZ response to hemispherically asymmetric forcings. *J. Climate*, **31**, 3659–3678, https://doi.org/10.1175/JCLI-D-17-0723.1.

Dessler, A. E., M. R. Schoeberl, T. Wang, S. M. Davis, and K. H. Rosenlof, 2013: Stratospheric water vapor feedback. *Proc. Natl. Acad. Sci. USA*, **110**, 18 087–18 091, https://doi.org/10.1073/pnas.1310344110.

Edmon, H. J., B. J. Hoskins, and M. E. McIntyre, 1980: Eliassen-Palm cross sections for the troposphere. *J. Atmos. Sci.*, **37**, 2600–2616, https://doi.org/10.1175/1520-0469(1980)037<2600:EPCSFT>2.0.CO;2.

Frierson, D. M. W., 2007: The dynamics of idealized convection schemes and their effect on the zonally averaged tropical circulation. *J. Atmos. Sci.*, **64**, 1959–1976, https://doi.org/10.1175/JAS3935.1.

——, 2008: Midlatitude static stability in simple and comprehensive general circulation models. *J. Atmos. Sci.*, **65**, 1049–1062, https://doi.org/10.1175/2007JAS2373.1.

Grise, K. M., and S. M. Davis, 2020: Hadley cell expansion in CMIP6 models. *Atmos. Chem. Phys.*, **20**, 5249–5268, https://doi.org/10.5194/acp-20-5249-2020.

Hassanzadeh, P., and Z. Kuang, 2016: The linear response function of an idealized atmosphere. Part I: Construction using Green's functions and applications. *J. Atmos. Sci.*, **73**, 3423–3439, https://doi.org/10.1175/JAS-D-15-0338.1.

Haynes, P. H., M. E. McIntyre, T. G. Shepherd, C. J. Marks, and K. P. Shine, 1991: On the "downward control" of extratropical diabatic circulations by eddy-induced mean zonal forces. *J. Atmos. Sci.*, **48**, 651–678, https://doi.org/10.1175/1520-0469(1991)048<0651:OTCOED>2.0.CO;2.

Held, I. M., 2000: *The General Circulation of the Atmosphere*. Geophysical Fluid Dynamics program, Woods Hole Oceanographic Institution, 70 pp., https://www.gfdl.noaa.gov/wp-content/uploads/files/user_files/ih/lectures/woods_hole.pdf.

——, 2019: 100 years of progress in understanding the general circulation of the atmosphere. *A Century of Progress in Atmospheric and Related Sciences: Celebrating the American Meteorological Society Centennial, Meteor. Monogr.*, No. 59, Amer. Meteor. Soc., 6.1–6.23, https://doi.org/10.1175/AMSMONOGRAPHS-D-18-0017.1.

——, and B. J. Soden, 2006: Robust responses of the hydrological cycle to global warming. *J. Climate*, **19**, 5686–5699, https://doi.org/10.1175/JCLI3990.1.

Hu, Y., and Q. Fu, 2007: Observed poleward expansion of the Hadley circulation since 1979. *Atmos. Chem. Phys.*, **7**, 5229–5236, https://doi.org/10.5194/acp-7-5229-2007.

IPCC, 2013: *Climate Change 2013: The Physical Science Basis*. T. F. Stocker et al., Eds. Cambridge University Press, 1535 pp.

James, I. N., 1987: Suppression of baroclinic instability in horizontally sheared flows. *J. Atmos. Sci.*, **44**, 3710–3720, https://doi.org/10.1175/1520-0469(1987)044<3710:SOBIIH>2.0.CO;2.

Kidston, J., and E. P. Gerber, 2010: Intermodel variability of the poleward shift of the austral jet stream in the CMIP3 integrations linked to biases in 20th century climatology. *Geophys. Res. Lett.*, **37**, L09708, https://doi.org/10.1029/2010GL042873.

——, and G. K. Vallis, 2012: The relationship between the speed and the latitude of an eddy-driven jet in a stirred barotropic model. *J. Atmos. Sci.*, **69**, 3251–3263, https://doi.org/10.1175/JAS-D-11-0300.1.

——, ——, S. M. Dean, and J. A. Renwick, 2011: Can the increase in the eddy length scale under global warming cause the poleward shift of the jet streams? *J. Climate*, **24**, 3764–3780, https://doi.org/10.1175/2010JCLI3738.1.

Kushner, P. J., and M. L. Polvani, 2004: Stratosphere–troposphere coupling in a relatively simple AGCM: The role of eddies. *J. Climate*, **17**, 629–639, https://doi.org/10.1175/1520-0442(2004)017<0629:SCIARS>2.0.CO;2.

Lau, W. K. M., and K.-M. Kim, 2015: Robust Hadley circulation changes and increasing global dryness due to CO_2 warming from CMIP5 model projections. *Proc. Natl. Acad. Sci. USA*, **112**, 3630–3635, https://doi.org/10.1073/pnas.1418682112.

Lee, S., and H.-K. Kim, 2003: The dynamical relationship between subtropical and eddy-driven jets. *J. Atmos. Sci.*, **60**, 1490–1503, https://doi.org/10.1175/1520-0469(2003)060<1490:TDRBSA>2.0.CO;2.

Lorenz, D. J., 2014: Understanding midlatitude jet variability and change using Rossby wave chromatography: Poleward-shifted jets in response to external forcing. *J. Atmos. Sci.*, **71**, 2370–2389, https://doi.org/10.1175/JAS-D-13-0200.1.

——, and D. L. Hartmann, 2001: Eddy–zonal flow feedback in the Southern Hemisphere. *J. Atmos. Sci.*, **58**, 3312–3327, https://doi.org/10.1175/1520-0469(2001)058<3312:EZFFIT>2.0.CO;2.

——, and E. T. DeWeaver, 2007: Tropopause height and zonal wind response to global warming in the IPCC scenario integrations. *J. Geophys. Res. Atmos.*, **112**, https://doi.org/10.1029/2006JD008087.

Lorenz, E. N., 1955: Available potential energy and the maintenance of the general circulation. *Tellus*, **7**, 157–167, https://doi.org/10.3402/tellusa.v7i2.8796.

Lu, J., G. A. Vecchi, and T. Reichler, 2007: Expansion of the Hadley cell under global warming. *Geophys. Res. Lett.*, **34**, L06805, https://doi.org/10.1029/2006GL028443.

——, G. Chen, and D. M. W. Frierson, 2008: Response of the zonal mean atmospheric circulation to El Niño versus global warming. *J. Climate*, **21**, 5835–5851, https://doi.org/10.1175/2008JCLI2200.1.

——, L. Sun, Y. Wu, and G. Chen, 2014: The role of subtropical irreversible PV mixing in the zonal mean circulation response to global warming–like thermal forcing. *J. Climate*, **27**, 2297–2316, https://doi.org/10.1175/JCLI-D-13-00372.1.

Manabe, S., and R. T. Wetherald, 1967: Thermal equilibrium of the atmosphere with a given distribution of relative humidity. *J. Atmos. Sci.*, **24**, 241–259, https://doi.org/10.1175/1520-0469(1967)024<0241:TEOTAW>2.0.CO;2.

Mbengue, C., and T. Schneider, 2017: Storm-track shifts under climate change: Toward a mechanistic understanding using baroclinic mean available potential energy. *J. Atmos. Sci.*, **74**, 93–110, https://doi.org/10.1175/JAS-D-15-0267.1.

Merlis, T. M., and M. Henry, 2018: Simple estimates of polar amplification in moist diffusive energy balance models. *J. Climate*, **31**, 5811–5824, https://doi.org/10.1175/JCLI-D-17-0578.1.

——, T. Schneider, S. Bordoni, and I. Eisenman, 2013: Hadley circulation response to orbital precession. Part I: Aquaplanets. *J. Climate*, **26**, 740–753, https://doi.org/10.1175/JCLI-D-11-00716.1.

Ming, Y., and I. M. Held, 2018: Modeling water vapor and clouds as passive tracers in an idealized GCM. *J. Climate*, **31**, 775–786, https://doi.org/10.1175/JCLI-D-16-0812.1.

Norris, J., G. Chen, and J. D. Neelin, 2019: Changes in frequency of large precipitation accumulations over land in a warming climate from the CESM large ensemble: The roles of moisture, circulation, and duration. *J. Climate*, **32**, 5397–5416, https://doi.org/10.1175/JCLI-D-18-0600.1.

O'Gorman, P. A., 2010: Understanding the varied response of the extratropical storm tracks to climate change. *Proc. Natl. Acad. Sci. USA*, **107**, 19 176–19 180, https://doi.org/10.1073/pnas.1011547107.

Paynter, D., and V. Ramaswamy, 2014: Investigating the impact of the shortwave water vapor continuum upon climate simulations using GFDL global models. *J. Geophys. Res. Atmos.*, **119**, 10 720–10 737, https://doi.org/10.1002/2014JD021881.

Previdi, M., and B. G. Liepert, 2007: Annular modes and Hadley cell expansion under global warming. *Geophys. Res. Lett.*, **34**, L22701, https://doi.org/10.1029/2007GL031243.

Ring, M. J., and R. A. Plumb, 2008: The response of a simplified GCM to axisymmetric forcings: Applicability of the fluctuation–dissipation theorem. *J. Atmos. Sci.*, **65**, 3880–3898, https://doi.org/10.1175/2008JAS2773.1.

Rivière, G., 2011: A dynamical interpretation of the poleward shift of the jet streams in global warming scenarios. *J. Atmos. Sci.*, **68**, 1253–1272, https://doi.org/10.1175/2011JAS3641.1.

Roe, G., 2009: Feedbacks, timescales, and seeing red. *Annu. Rev. Earth Planet. Sci.*, **37**, 93–115, https://doi.org/10.1146/annurev.earth.061008.134734.

Scheff, J., and D. M. W. Frierson, 2012: Robust future precipitation declines in CMIP5 largely reflect the poleward expansion of model subtropical dry zones. *Geophys. Res. Lett.*, **39**, L18704, https://doi.org/10.1029/2012GL052910.

Seidel, D. J., Q. Fu, W. J. Randel, and T. J. Reichler, 2008: Widening of the tropical belt in a changing climate. *Nat. Geosci.*, **1**, 21–24, https://doi.org/10.1038/ngeo.2007.38.

Shaw, T. A., 2019: Mechanisms of future predicted changes in the zonal mean mid-latitude circulation. *Curr. Climate Change Rep.*, **5**, 345–357, https://doi.org/10.1007/s40641-019-00145-8.

Simpson, I. R., and L. M. Polvani, 2016: Revisiting the relationship between jet position, forced response, and annular mode variability in the southern midlatitudes. *Geophys. Res. Lett.*, **43**, 2896–2903, https://doi.org/10.1002/2016GL067989.

Sun, L., G. Chen, and J. Lu, 2013: Sensitivities and mechanisms of the zonal mean atmospheric circulation response to tropical warming. *J. Atmos. Sci.*, **70**, 2487–2504, https://doi.org/10.1175/JAS-D-12-0298.1.

Tao, L., Y. Hu, and J. Liu, 2016: Anthropogenic forcing on the Hadley circulation in CMIP5 simulations. *Climate Dyn.*, **46**, 3337–3350, https://doi.org/10.1007/s00382-015-2772-1.

Thompson, D. W. J., S. Solomon, P. J. Kushner, M. H. England, K. M. Grise, and D. J. Karoly, 2011: Signatures of the Antarctic ozone hole in Southern Hemisphere surface climate change. *Nat. Geosci.*, **4**, 741–749, https://doi.org/10.1038/ngeo1296.

Vallis, G. K., P. Zurita-Gotor, C. Cairns, and J. Kidston, 2015: Response of the large-scale structure of the atmosphere to global warming. *Quart. J. Roy. Meteor. Soc.*, **141**, 1479–1501, https://doi.org/10.1002/qj.2456.

Waugh, D. W., and Coauthors, 2018: Revisiting the relationship among metrics of tropical expansion. *J. Climate*, **31**, 7565–7581, https://doi.org/10.1175/JCLI-D-18-0108.1.

Williams, G. P., 2006: Circulation sensitivity to tropopause height. *J. Atmos. Sci.*, **63**, 1954–1961, https://doi.org/10.1175/JAS3762.1.

Wright, J. S., A. Sobel, and J. Galewsky, 2010: Diagnosis of zonal mean relative humidity changes in a warmer climate. *J. Climate*, **23**, 4556–4569, https://doi.org/10.1175/2010JCLI3488.1.

Wu, Y., M. Ting, R. Seager, H.-P. Huang, and M. A. Cane, 2011: Changes in storm tracks and energy transports in a warmer climate simulated by the GFDL CM2.1 model. *Climate Dyn.*, **37**, 53–72, https://doi.org/10.1007/s00382-010-0776-4.

——, R. Seager, M. Ting, N. Naik, and T. A. Shaw, 2012: Atmospheric circulation response to an instantaneous doubling of carbon dioxide. Part I: Model experiments and transient thermal response in the troposphere. *J. Climate*, **25**, 2862–2879, https://doi.org/10.1175/JCLI-D-11-00284.1.

Yin, J. H., 2005: A consistent poleward shift of the storm tracks in simulations of 21st century climate. *Geophys. Res. Lett.*, **32**, L18701, https://doi.org/10.1029/2005GL023684.